Mapping Nucleosome Locations on the 208−12 by AFM Provides Clear Evidence for Cooperativity in Array Occupation †

ARTICLE *in* BIOCHEMISTRY · APRIL 2002

Impact Factor: 3.02 · DOI: 10.1021/bi011612e · Source: PubMed

5 AUTHORS, INCLUDING:

Jaya Yodh
University of Illinois, Urbana-Champaign
22 PUBLICATIONS **405** CITATIONS
SEE PROFILE

Neal W Woodbury
Arizona State University
138 PUBLICATIONS **4,065** CITATIONS
SEE PROFILE

Szilvia Luda
Corvinus University of Budapest
72 PUBLICATIONS **2,939** CITATIONS
SEE PROFILE

Yuri L. Lyubchenko
University of Nebraska Medical Center
192 PUBLICATIONS **5,608** CITATIONS
SEE PROFILE

Mapping Nucleosome Locations on the 208-12 by AFM Provides Clear Evidence for Cooperativity in Array Occupation†

Jaya G. Yodh,[‡,§] Neal Woodbury,[§,||] Luda S. Shlyakhtenko,[⊥] Yuri L. Lyubchenko,[#] and D. Lohr*[,||]

Division of Basic Sciences, Midwestern University, Arizona College of Osteopathic Medicine, Glendale, Arizona 85308, Department of Chemistry and Biochemistry, Arizona State University, P.O. Box 871604, Tempe, Arizona 85287-1604, Department of Microbiology, Arizona State University, Tempe, Arizona 85287-2701, and Department of Microbiology and Department of Biology, Arizona State University, Tempe, Arizona 85287-1501

Received August 6, 2001

ABSTRACT: Concatameric sea urchin 5S rDNA templates reconstituted with histones provide very popular chromatin models for many kinds of in vitro studies. We have used AFM to characterize the locational aspects of nucleosome occupation on one such array, the 208-12, by determining the internucleosomal- and end-distance distributions for arrays reconstituted to various subsaturating levels with nonacetylated or hyperacetylated HeLa histones. A simulation analysis of the experimental distributions confirms the qualitative conclusions and provides quantitative parameter values for the identified features. For *nonacetylated* arrays, the end-distance data demonstrate the nucleosome positioning ability of the 5S sequence and detect an enhanced preference for nucleosomes to bind at DNA termini. The internucleosomal-distance data provide clear evidence for cooperativity in nucleosome location on these templates, detectable even at subsaturated loading levels. *Hyperacetylated* arrays show no change in the preference of nucleosomes to bind at termini and a slight change in nucleosome positioning behavior but, most strikingly, little or no evidence for cooperativity in nucleosome location. Thus, acetylation of the N-terminal histone tails abolishes the cooperativity.

The basic level of structural organization in eukaryotic chromosomes is the nucleosomal array, which consists of multiple core nucleosomes spaced by varying lengths of linker DNA. The relative spacing arrangement of core nucleosomes in chromosomal arrays has been a question of considerable interest since the earliest days of chromatin analysis (cf. *1*−*4*).

One of the most popular model systems for in vitro studies of nucleosomal arrays are the concatameric 5S rDNA[1] templates developed by Simpson et al. (*5*). Each 5S unit, e.g., the 208 bp unit, has the ability to position a nucleosome (*6*) in a major frame and a set of minor frames that conserve the rotational setting of the nucleosome on the DNA, i.e., positions that vary by multiples of the DNA helical repeat (*7, 8*). Concatamers of these 5S units, such as the dodecameric repeat referred to as the 208-12, provide a template that can be reconstituted into defined polynucleosomal arrays suitable for biophysical and biochemical studies. Nucleosome reconstitution on these concatameric 5S templates follows the same order of histone assembly as chromatin assembled in vivo (*9*), and for this and other reasons, these in vitro reconstituted arrays are thought to be valid models for the nucleosomal arrays that form the basic structural organization of eukaryotic chromosomes (cf. *10*).

The many published studies that have analyzed the structural properties of 5S arrays have focused mainly on conformational issues: chromatin folding or compaction (*9, 11*); how folding depends on core histone tails, acetylation (*12*−*15* and references cited therein), or linker histones (*16*−*18*); how folding affects transcription or transcription factor binding to chromatin (*19*−*21*). Our labs have been interested in other biophysical features, specifically how nucleosomes populate these templates. Such studies can provide insight on the fundamental nature of polynucleosomal occupation on multi-binding-site DNA templates, answering such questions as whether occupation is a random process, whether there is cooperativity, etc. Subsaturated arrays, i.e., arrays containing fewer nucleosomes than the number of nucleosome binding sites available in the DNA template, provide a very useful system for these types of studies because of the occupancy choices available to nucleosomes loading onto such arrays. Subsaturated arrays also have intrinsic interest as models for important regulatory regions such as replication origins (*22, 23*) and gene promoters (cf. *24*), which are often not fully saturated with nucleosomes.

Our experimental approach utilizes atomic force microscopy (AFM). AFM is a powerful imaging technique that can be used to visualize many types of nucleic acid and

† Support to Y.L.L. (GM54991) and D.L. (CA-85990) from the NIH is gratefully acknowledged.

* To whom correspondence should be addressed. Fax: 480-965-2747, e-mail: dlohr@asu.edu.

‡ Division of Basic Sciences, Midwestern University, Arizona College of Osteopathic Medicine.

§ These authors contributed equally to this work.

|| Department of Chemistry and Biochemistry, Arizona State University.

⊥ Department of Microbiology, Arizona State University.

Department of Microbiology and Department of Biology, Arizona State University.

[1] Abbreviations: AFM, atomic force microscopy; bp, base pair(s); rDNA, ribosomal DNA.

10.1021/bi011612e CCC: $22.00
Published on Web 02/16/2002

nucleoprotein complexes (cf. *25, 26*), including chromatin isolated from cells (*27*−*30*) or reconstituted in vitro (*31*−*33*). AFM offers important advantages for the types of investigations described in this paper. The ability to directly visualize individual templates allows one to count precisely the number of nucleosomes present and to determine the location of each nucleosome on the template. By analyzing many molecules, the real behavior of any experimental property of interest, such as the distribution of internucleosomal-distances, can be obtained. The experimental behavior can then be compared to theoretical models for insights on the occupation properties of nucleosomes on these multisite templates.

Previously, we analyzed the population distributions, i.e., the fraction of templates containing *n* nucleosomes as a function of *n*, for 208-12 subsaturated arrays (*33*) and for 172-12 subsaturated arrays (*61*), reconstituted with nonacetylated or hyperacetylated histones. In the work described here, we characterize the locational aspects of nucleosome occupation on nonacetylated and hyperacetylated 208-12 subsaturated nucleosomal arrays. This comparison is important because of the strong association of histone acetylation with the processes of transcription and replication (*34*−*38*). Acetylation occurs at specific lysine residues (*39*) located in the N-terminal tails of the core histones. These tails project out from the globular portion of the nucleosome (*40, 41*) and have been suggested to mediate internucleosomal contact and chromatin compaction (*10, 41, 42*). We find evidence for specific nucleosome positioning within the 208 bp unit, as expected, and a distinct preference for nucleosome occupation at DNA termini in both acetylated and unacetylated arrays. Most importantly, we find strong evidence for cooperativity in the occupation of these templates, but only in nonacetylated chromatin. Acetylated arrays show no evidence of cooperativity.

EXPERIMENTAL PROCEDURES

Measuring Nucleosome Locations on the 208-12 Templates. 208-12 DNA and HeLa histone isolation, chromatin reconstitution, glutaraldehyde fixation, deposition onto mica, and AFM imaging were done as described previously (*33*). The DNA templates used contain 12 tandem, head-to-tail 208 bp repeat units, plus ∼30 bp of non-5S DNA at the origin (head) end of repeat 1 and 6 bp beyond the tail end of repeat 12 (J. Hansen, private communication). For the analysis of distances, each molecule was traced from one end to the other, recording the following: (i) the distance from one template terminus to the proximal edge of the first nucleosome ("1") encountered; (ii) the width of nucleosome 1; (iii) the distance from the distal edge of nucleosome 1 to the proximal edge of the next nucleosome (i.e., 2) encountered; (iv) the width of nucleosome 2; [repeat steps (iii) and (iv) for all internal nucleosomes]; (v) the distance from the distal edge of the terminal nucleosome to the other template terminus. The data were divided into "end- " and "internucleosomal"-distances ("E" and "I", Figure 1) and pooled. End-distances, of which there will be two per molecule, are the distances from each template terminus to the first nucleosome encountered. Internucleosomal-distances are the distances between nucleosomes.

To perform the measurements, AFM images of nucleosomal arrays were converted from nanoscope format (Digital Instruments, Inc.) into TIF files and the measurements made using Scion (NIH Image) software. In each field of a given reconstituted sample, we counted every molecule possible, to avoid bias in the data set. To be used, a molecule had to have discernible ends and distinguishable nucleosomes and thus be clearly traceable from one end to the other. Each molecule analyzed was marked in order to avoid remeasuring it. As an internal check, contour lengths for each molecule were also recorded. The contour length varies slightly among molecules but decreases as the number of nucleosomes present on the molecule increases, as expected.

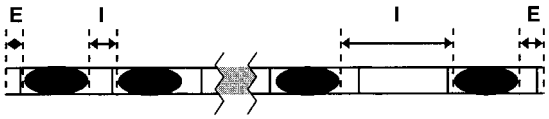

FIGURE 1: End-distances versus internucleosomal-distances. An arrangement of nucleosomes, represented as ovals, is depicted on the 208-12 DNA template. Individual 208 bp DNA units are demarcated by solid vertical lines. E = end-distance, I = internucleosomal-distance.

We measured each type of distance in two ways: by measuring to the nucleosome edge or to the nucleosome center. The center of a nucleosome was deemed to lie at 1/2 of the nucleosome width from the edge, on the line connecting the DNA entry and exit sites on the nucleosome. For the end-distances, values are given by the quantities (i) or (v) above for edge-to-terminus measurements or by the sum of steps [(i) + 0.5 × (ii)] or [0.5 × (the terminal nucleosome width + (v)] for center-to-terminus measurements. For internucleosomal-distances, edge-to-edge values for each nucleosome are given by the quantities in steps (iii) and center-to-center values by the sum of the steps [0.5 × (ii) + (iii) + 0.5 × (iv)]. Note that the center-to-center (and terminus-to-center) distances contain the nucleosome half-widths for the precise pair (or terminal nucleosome) whose separation is being measured, i.e., the relevant local values and not average values.

We analyzed three groups of reconstituted samples based on their level of array subsaturation or n_{av} value: $n_{av} = 3-4$, $n_{av} = 5-6$, $n_{av} = 8-9$. These groups were chosen because those loading levels showed interesting (nonrandom), n_{av}-dependent behavior in the population distribution analysis (*33*; *61*) and because this range contains enough nucleosomes to detect interesting behavior and yet not too many, which would complicate counting by AFM techniques (*33*). For each range of subsaturation, 50−150 molecules in each of 3 independent reconstituted samples were measured. The data from each reconstitute were initially sorted by nucleosome loading level or *n* value, i.e., all of the arrays with 5 bound nucleosomes in one set, those with 6 bound nucleosomes in another, etc. This allowed us to test for *n* dependence in the locational features. (There was none; see below.) For the major analysis of the data, the experimentally measured distances from all *n* values/all samples were combined and sorted into bins. The bin size used was 20.8 bp (7.07 nm), which has the effect of dividing the 208 bp repeat unit into 10 bins, a division that seems appropriate to the accuracy of the data and yet provides reasonable detail. This is the bin size used to generate the histograms in Figures 3−5 and is also used in the simulation analysis described below.

Simulation of the Nucleosome Location Data. A Monte Carlo approach was employed to carry out a quantitative simulation using the experimentally determined nucleosome location data. The simulation was carried out by assigning each bin a fractional likelihood of being occupied by a nucleosome. An occupation (binding) site is considered to start at the position of the nucleosome edge closest to the origin of the 208 bp DNA unit and to extend for 147 bp downstream (toward the opposite end of the template). The relative likelihood of nucleosome binding at any given site is allowed to depend on several factors. First, there is the random probability of occupation, i.e., random statistics, and steric effects, i.e., two nucleosomes cannot overlap each other on the DNA. The second factor is binding enhancement at particular positions within the 208 bp unit that occurs as a result of nucleosome positioning tendencies intrinsic to the 208 bp DNA. Third, contributions due to the proximity of other bound nucleosomes are considered (binding cooperativity). Finally, the distance from the terminus of the DNA fragment is also allowed to modify the likelihood of occupation in bins close to the DNA ends, i.e., end effects. Thus, the simulation consists of a linear array of bins, each of which has a particular relative nucleosome occupancy depending on the above four factors.

To carry out the simulation, nucleosomes are added (through random number generation weighted by the relative occupancy) to the template. As they are added, the binding landscape changes, and the array of binding constants is recalculated, changing the weighting used with the random number generation for selection of the next binding site. A simulation consists of sequentially loading up to $n = 10$ nucleosomes (the highest number counted experimentally) onto a template in this way. After each nucleosome is loaded, the positions are determined and stored. This whole process is repeated 5000 times, generating 5000 loaded fragments for each value of n between 2 and 10. This data set is analyzed and displayed just as the experimental data.

The simulation yields 10 (relative) binding constants, 1 for each of the 10 bins in the 208 bp unit. These constants are considered to be invariant from one 208 bp repeat to the next and represent the sequence dependence of nucleosome binding, i.e., positioning, within the 208 bp repeat unit. Also, there are 10 factors describing the distance dependence of cooperativity. These cooperativity factors are applied to all the bins that lie within one 208 bp repeat unit (10 bins) of the closest edge of each bound nucleosome and thus reflect nearest-neighbor effects only. Finally, there are an additional 10 relative binding factors applied to the 10 bins nearest the absolute termini of the DNA fragment. These test for relative enhancements associated with binding at the DNA ends. Since we could not tell the difference in our measurements between the two ends of the DNA, the enhanced end binding was only applied to the "left" end of the DNA, but clearly could represent binding to either end.

The goal of the simulation was to determine the parameter values that lead to the best "fit" to the experimental data, for the various parameters listed above. To arrive at a good initial guess, the parameters were first varied over a fairly large range by hand. This can produce simulated distributions that closely approximate the experimental distributions. The simulations were then fine-tuned by allowing the computer to adjust parameters systematically, varying them, one, two, or three at a time. The size of the calculated fragment set had to be limited due to constraints on calculation time in the computer and the desire to search over as large a region of parameter space as possible. The goodness of the final fit was determined by calculating a reduced global chi squared error. This was calculated by comparing the fit to the data globally, both for the end-distance data and for the internucleosomal data at each of the $n = 2$ through 10 loadings. Note that for the fits, the results from different loadings were not summed, but considered separately in a large global analysis. For the fits shown in Figure 7, the global chi squared errors were all between 0.9 and 1.15, showing that the fits were as good overall as the statistics would allow (a reduced chi squared near 1.0 means the error between the fit and the data is within the noise). With the exception of the end effects, it was also possible to arrive at essentially the same model parameters by performing the systematic variation starting with a purely random binding model and letting the computer completely determine the binding parameters, by fitting the simulation against the experimental data. The end effects are only observed in the nucleosomal bin closest to the end of the DNA; the effect of an error in that one bin was not large enough to allow an accurate determination of the simulation parameters by systematic variation. This is because the simulation itself had error associated with it (determined by the number of fragments calculated and used in determining the simulated curve).

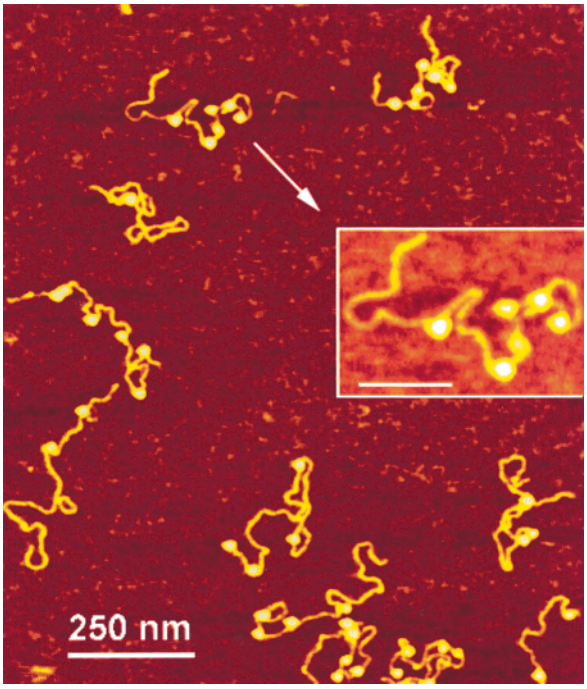

FIGURE 2: Typical AFM image used for the distance measurements. $n_{av} = 4.1$ for this nonacetylated reconstitute. The inset shows a magnified image of the individual molecule indicated. The bar in the inset represents 100 nm.

RESULTS

Figure 2 shows an example of the type of AFM image used in the analyses described below. The array molecules are quite clearly visualized and the fields free of extraneous material. More fields and the population distributions for these arrays can be seen elsewhere (*33*). To characterize the nucleosome locational features on these templates, the data

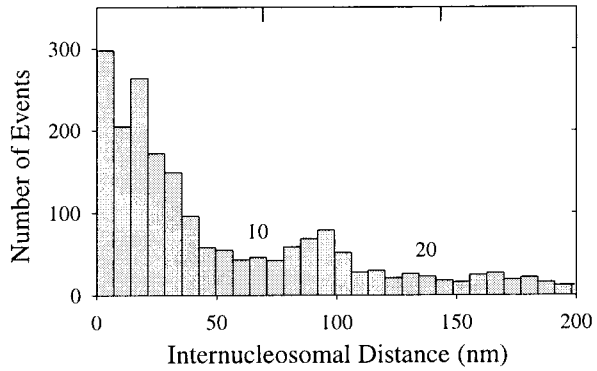

FIGURE 3: Composite internucleosomal-distance distributions for nonacetylated 208-12 subsaturated arrays. This histogram presents a compilation of all measured internucleosomal nearest-neighbor separations, i.e., all molecules/all *n* values/all samples, measured as nucleosome edge-to-edge distances. The *x*-axis is distance in nm, and the data are presented as ~7 nm (~20 bp) wide bins. The *y*-axis is the number of times a particular internucleosomal-distance represented by each of the bins occurs in the data set. For ease of reference, every 10th bin (208 bp worth of DNA) is labeled, and tic marks are placed along the top horizontal axis.

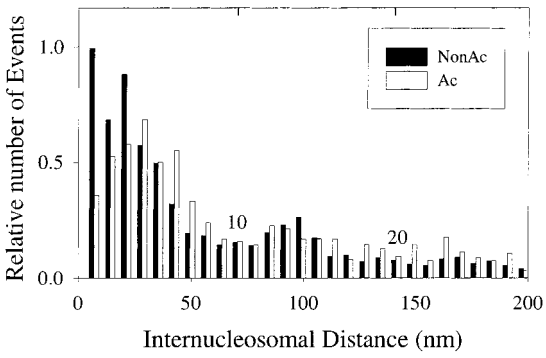

FIGURE 4: Internucleosomal-distance distributions for acetylated versus nonacetylated 208-12 subsaturated arrays. The histograms again present the compilation of all measured internucleosomal separations, all molecules/all *n* values/all samples, measured as edge-to-edge distances. White bars denote acetylated samples, and the dark bars denote nonacetylated samples. The *x*-axis is distance in nm, divided into ~7 nm wide bins, and the *y*-axis is the relative frequency of occurrence for the particular internucleosomal-distance represented by each of the bins. For ease of reference, every 10th bin (208 bp worth of DNA) is labeled, and tic marks are placed along the horizontal axis.

were analyzed as (i) internucleosomal-distances, i.e., the distances between nucleosome nearest neighbors on the template, and (ii) end-distances, the distances from the terminal nucleosome on each end to the adjacent template terminus. The two DNA termini are not distinguishable from each other in the images; thus, both end-distances are binned together. The two termini differ slightly in the amounts of non-208-12 DNA associated with each, 30 bp at the head end of repeat 1 and 6 bp at the tail end of repeat 12 (J. Hansen, private communication), and in the orientation of the 208 bp unit, which will place the major nucleosome positioning frame(s) at different relative locations with respect to the two termini. Thus, there is some ambiguity in the end-distance analysis. On the other hand, the internucleosomal-distance analysis is not sensitive to the nonequivalence of DNA ends and thus lacks such ambiguity.

I. Experimental Distributions

(A) Internucleosomal-Distances. We initially determined distance distributions separately for each of the various *n* classes ($n = 3, 4, 5$, etc. nucleosomes), in individual samples or in pools of samples at various average loading levels. That approach provided little useful information, except to confirm that the distributions become more compact, i.e., shift to lower distances, as the number of nucleosomes on the template increases, as they should (not shown). Therefore, we analyzed the data as a composite set, i.e., the sum of all molecules/all nucleosome loading levels/all samples. Summing the data in this way has the advantage of increasing its statistical accuracy (which is limited simply by the number of fragments imaged and measured) and also provides more stringent criteria for perceived features than can be provided by individual distributions.

The composite internucleosomal-distance distribution for 208-12 subsaturated chromatin arrays reconstituted with nonacetylated histones is shown in Figure 3. The data are presented as a histogram in which the number of nucleosome neighbors lying at a given distance from one another is plotted against distance. Distances are pooled into and displayed as 7 nm (~20 bp) wide bins. Based on the known nucleosome positioning preferences of the 208 bp sequence, one would expect to observe distinct periodicity in this distribution, reflecting the regular recurrence of positioning frames along the multisite template. While there is some periodicity in the distribution, it is not very pronounced, suggesting that effects in addition to positioning preferences within the 208 bp unit contribute to determining internucleosomal distances in these 208-12 chromatin arrays. The nature of at least one of these other contributions is suggested by careful analysis of Figure 3. The data show that there is a significant number of molecules in the first bin, which corresponds to internucleosomal distances of 0−7 nm (0−20 bp), i.e., nucleosomes located very close together on the 208-12 template. Indeed, bin 1 is the most populated bin in the distribution, indicating that location of two nucleosomes very close to one another is a favored state. The average internucleosomal separation on these templates would be expected to be ~60 bp, the difference between the DNA repeat of 208 bp and the 147 bp length of DNA covered by a nucleosome, which would correspond to bins 3−4. The preponderance of much shorter internucleosomal separations in the distribution indicates that there is cooperativity in nearest-neighbor nucleosome location on these templates.

Further insight on this feature is obtained from an analysis of the internucleosomal-distance distributions from acetylated 208-12 arrays (Figure 4). The most populated bin in the acetylated distribution is bin 4, corresponding to an internucleosomal separation of ~60−80 bp, which is close to the expected average value. Bin 1, which reflects close nucleosome neighbors, is the least populated of the first six bins (Figure 4), and these short separations are no more common than very long internucleosomal separations, ~100−120 bp (bin 6) and ~120−140 bp (bin 7). Thus, acetylated chromatin arrays do not show an enhancement in the numbers of molecules with short internucleosomal distances, and therefore nucleosomes located near one another are not a preference in these arrays. This is in striking contrast to the nonacetylated distribution, wherein bins 1, 2, and 3 are the most populated and long internucleosomal separations,

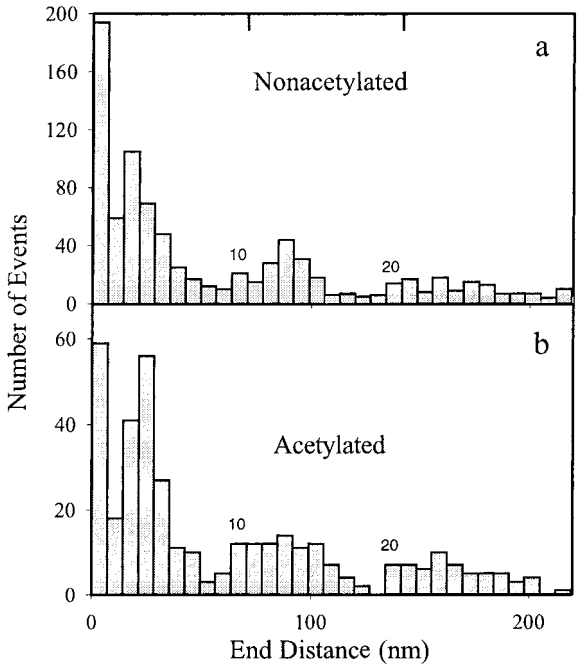

FIGURE 5: Composite end-distance distributions. These histograms present the compilation of the end-distance data (template terminus to nucleosome edge distances) for all molecules/all *n* values/all samples. Panel a shows the data for nonacetylated histone reconstitutes and panel b for acetylated reconstitutes. The *x*-axis represents distances, pooled and displayed as 7 nm wide bins, and the *y*-axis represents the number of times a particular end-distance within the distance range represented by each of the bins was observed. For ease of reference, every 10th bin (208 bp worth of DNA) is labeled, and tic marks are placed along the horizontal axis.

corresponding to ~100−120 bp (bin 6) and ~120−140 bp (bin 7), are uncommon. This comparison demonstrates that cooperativity in nucleosome location is a property of nonacetylated nucleosomal arrays; acetylation of the histone tails removes the cooperative effects. Therefore, the cooperativity observed in nonacetylated chromatin must arise from a histone tail-mediated effect, probably internucleosomal contact. The precise stage(s) in the reconstitution process that is (are) cooperative remains unknown.

Traditionally, interparticle distances in AFM are measured as center-to-center distances, to minimize errors arising from the tip dilation effect, i.e., the broadening of particle sizes and particle boundaries due to the finite (and variable) widths of the tips used in AFM studies (*25*, *43*). Therefore, we also determined the center-to-center internucleosomal distance distributions for these arrays. These data yield similar conclusions regarding cooperativity in nucleosome location as the edge-to-edge results described above (not shown).

The data in Figure 4 also suggest that the weak periodic peaks are somewhat broader in the acetylated than in the nonacetylated distributions. This feature could reflect the lack of cooperativity in the relative locations of neighboring nucleosomes in acetylated arrays, less defined positioning in the acetylated templates (see below), or loosening of the DNA at the termini of acetylated nucleosomes, a suggested effect of acetylation (reviewed in *44*). Again, center-to-center measurements show the same results (not shown).

(B) End-Distances. Figure 5 shows the composite end-distance histograms for subsaturated 208-12 nonacetylated (Figure 5a) or acetylated (Figure 5b) chromatin arrays. A striking feature in both distributions is the predominance of near zero end-distances (0−7 nm bin, Figure 5a,b). This feature reflects a preference for nucleosomes to be found at the template termini and suggests that nucleosomes have an enhanced affinity for the ends of the DNA fragment. We note that in the distributions from individual samples there is a progressive shift toward shorter end-distance values as the numbers of nucleosomes on the templates increase (not shown). This behavior reflects an increasing likelihood for the terminal 208 bp units to be occupied as loading levels increase and is the type of progression that would be expected.

A major feature of the 208 bp DNA sequence is its ability to position nucleosomes. Therefore, an important criterion for the AFM approach is whether it can detect nucleosome positioning in these templates and, if so, what position(s) within the 208 bp repeat is (are) preferred. The clearest evaluation of positioning is provided by (the nonzero peaks in) the end-distance measurements. The histograms in Figure 5 confirm that the locations of nucleosomes on these templates are not random; nucleosomes tend to occupy particular positions within the 208 bp DNA unit. Moreover, these preferred regions recur along the DNA at roughly the 208 bp repeat length of the template, i.e., every 10 bins. The distributions from acetylated chromatin are similar to those from nonacetylated chromatin. The slight quantitative differences between the two will be discussed below. Terminus-to-center distances yield similar conclusions (not shown). We note that the regularity of nucleosome location may in reality be greater than it appears to be because these histograms combine information from both (nonequivalent) ends.

II. Simulated Distributions: Quantitative Analyses of the AFM Results

In addition to the qualitative trends detected in Figures 3−5, quantitative information can be extracted by carrying out a simulation analysis of these data. This analysis uses the experimental results as a guide to obtain simulated fits to the experimental distributions. From the simulated fits, quantitative parameter values can be obtained, providing answers to several types of questions. Which positions in the 208 bp repeat are most favorable for nucleosome binding? How strong is the relative affinity for nucleosome binding at each of these positions and at DNA termini? What is the cooperativity coefficient for binding of two adjacent nucleosomes, and how far apart can they be and still experience cooperative effects?

As described under Experimental Procedures, the simulation includes as parameters: (1) position-dependent nucleosome binding constants within the 208 bp DNA unit; (2) distance-dependent cooperativity coefficients, i.e., internucleosomal effects that depend on the relative distances between nucleosome pairs; and (3) possible binding enhancements at the DNA termini. How each of the various effects alters the shape of a (simulated) distribution is illustrated in Figure 6 for the end-distances (panels a−c) and for the internucleosomal-distances (panels e−g). Obviously, a random loading process (no positioning preference, no

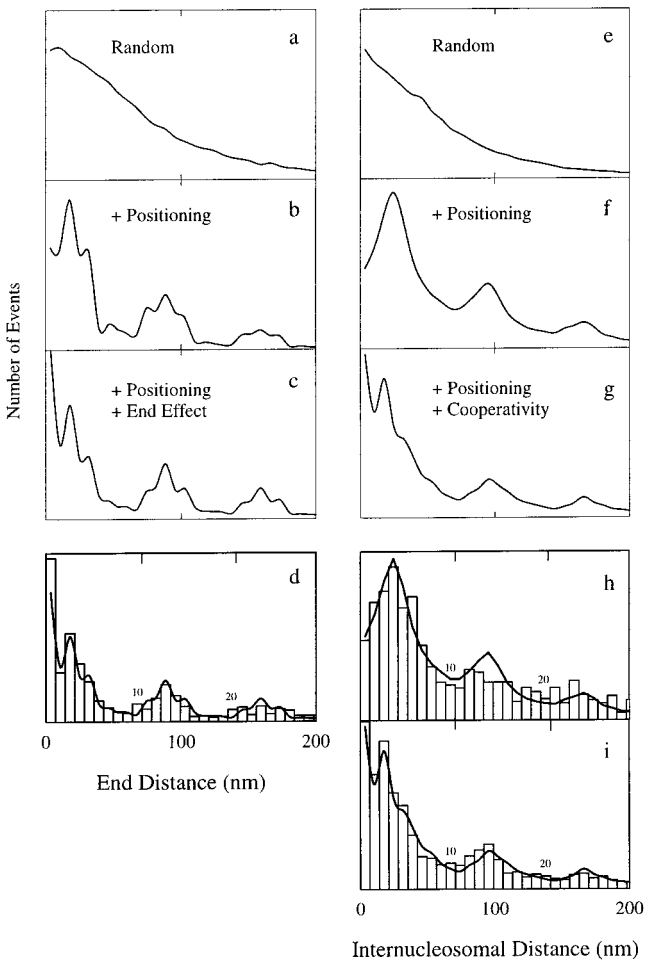

FIGURE 6: Effect of various features on the distribution profile, as determined from simulation analysis. The results of including combinations of the various types of preferences in a simulation are illustrated: (1) *positioning*: preferred binding position(s) within the 208 bp repeat; (2) *cooperativity*: binding effects between neighboring nucleosomes, as a function of their distance apart; (3) *end effects*: enhanced binding at DNA termini. The simulated distributions of end-distance measurements are shown in panels a−c for a random distribution (panel a), plus positioning (panel b) and plus positioning plus end preferences (panel c). Panel d compares the simulation in panel c to the experimental end-distance distribution (template terminus-to-edge distances, nonacetylated chromatin, Figure 5a). The simulated distributions of internucleosomal-distances are shown in panels e−g for a random distribution (panel e), plus positioning (panel f) and plus positioning plus cooperativity (panel g). Panels h and i compare the simulations of panels f and g to the experimental internucleosomal-distance distributions (Figure 4) for acetylated (panel h) and nonacetylated (panel i) chromatin arrays.

cooperativity, no end preference; panel a, Figure 6) does not resemble the experimental end-distance distribution at all (cf. Figure 5a). Including nucleosome positioning effects within the 208 bp repeat unit introduces periodicity into the distribution (panel b). Such periodicity is a major feature of the experimental distribution. As would be expected, allowing enhanced binding at DNA termini increases the population of templates with very short end-distances (panel c). The end-distance data for either acetylated or nonacetylated chromatin arrays can only be fit when enhanced binding to DNA termini is included in the model. The fit between the simulated distribution (including positioning and end preferences) and the experimental histogram (Figure 5a, nonacetylated chromatin) is illustrated in panel d. The inclusion of cooperativity has no detectable effect on the end-distance distribution (not shown).

For the internucleosomal-distance data, a random model again does not resemble the experimental results at all (panel e). The inclusion of positioning effects within the 208 bp repeat (panel f) produces a distribution that has periodicity but a low population of nucleosomes at very close internucleosomal distances, i.e., 0−20 bp. This distribution in fact resembles quite closely the internucleosomal-distance distribution from acetylated 208-12 chromatin arrays (panel h). Addition of cooperativity (panel g) increases the frequency of close-contacting nucleosomes and produces a distribution that resembles the data from nonacetylated chromatin (panel i). The inclusion of end-effects has little effect on the fit of the internucleosomal-distance data (not shown). Thus, the model simulations confirm the qualitative observations from the experimental data in Figures 3−5.

From the best fit simulations, quantitative parameter values were extracted (Figure 7):

(i) The top panels (a and b) rank the nucleosome binding positions within the 208 bp repeat. For unacetylated chromatin, there are three nearly equally preferred positions, with nucleosome occupation starting at ∼20, 40, and 60 bp (7, 14, and 21 nm) from the origin (nucleotide 1) of the 208 bp unit. There does not appear to be significantly enhanced binding elsewhere within the 208 bp unit. For acetylated nucleosomes, there are four preferred positions instead of three as in the nonacetylated samples. The slight differences in relative affinities for the preferred positions in acetylated and nonacetylated chromatin may not be significant.

(ii) Cooperativity in binding is strongest for pairs of nucleosomes in sites that are 0−20 bp apart on the template but is still detectable when nucleosomes are separated by up to 21 nm (∼60 bp) of template DNA (panel c). As noted above, cooperativity is a characteristic of nonacetylated chromatin; the acetylated chromatin distributions can be fit without cooperative effects. Indeed, the simulation detects no evidence for cooperativity in the acetylated samples (panel d).

(iii) Binding within 20 bp (7 nm) of the DNA termini is enhanced compared to nontermini binding, in both acetylated and nonacetylated reconstitutes (panels e and f). It is not possible to determine from these data whether there is an enhanced preference for one terminus or the other.

To check for loading level dependent differences in the distributions, we ran a simulation using data for molecules containing only lower loading levels, $n = 4$, 5, and 6, or only higher levels, $n = 7$, 8, and 9. We could detect no significant differences between these two sets and no significant differences versus the combined set (not shown). Thus, we conclude that the distance distribution features are loading level independent, in contrast to the population distribution features, which demonstrate definite loading level dependence (*33*).

DISCUSSION

We have used AFM to characterize the locational features of nucleosomes on subsaturated 208-12 polynucleosomal arrays. The experimental internucleosomal- and end-distance distributions suggest three major qualitative conclusions, which are confirmed and quantified by simulation analyses.

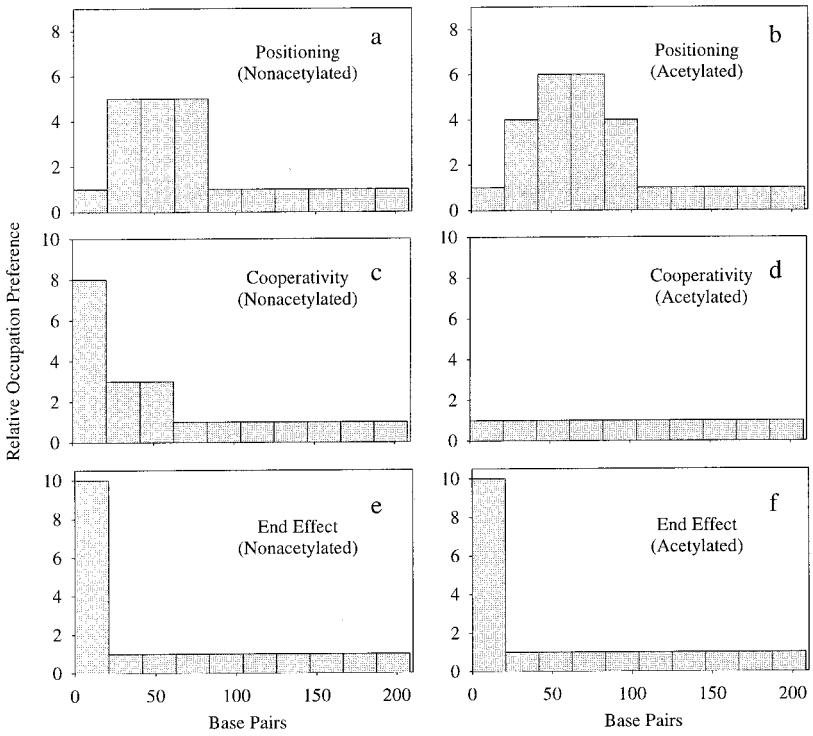

FIGURE 7: Quantitative parameter values from simulation analysis. Panels a (nonacetylated) and b (acetylated) display the relative binding constants for nucleosomes, i.e., positioning preferences within the 208 bp repeat. Panels c (nonacetylated) and d (acetylated) display the relative cooperativity coefficients for nucleosomes 0−7 nm (∼0−20 bp), 7−14 nm (∼20−40 bp), etc. apart on the 208-12 template. Panels e (nonacetylated) and f (acetylated) display the end preferences for the various bins on the terminal 208 bp unit(s). In this figure, the *x*-axis is base pairs; the individual bins are ∼20 bp wide. The *y*-axis is relative strength of the feature (in arbitrary units).

First, nucleosomes prefer binding to particular regions of the 208 bp repeat unit; i.e., nucleosomes show clear positioning preferences within this sequence. Previous studies have placed the major nucleosome positioning frame on the 208 bp sequence at 20−166 bp (a mononucleosomal template; *6*) or at 1−146 or 6−151 bp (polynucleosomal templates; *7, 8*). Our analysis suggests that nucleosomes prefer binding, about equally, in frames that initiate at ∼20, 40, and 60 bp from nucleotide 1, i.e., ∼20−166, ∼40−186, and ∼60−206 bp, respectively, on the 208 bp unit. In addition to being the major positioning frame in one analysis (*6*), the 20−166 bp frame was the most favored minor frame in another (*7*); 40−186 and 60−206 bp also were prominent minor frames in that work. Thus, AFM analysis detects many of the same positioning preferences seen in previous studies but suggests a somewhat different mix of preferred positions. The previous analyses all used nuclease digestion methods [DNase I (*6*) or MNase (*7, 8*)] to map nucleosome positions. AFM provides a different approach, one that avoids potential pitfalls associated with nuclease digestion analyses. However, the level of precision in frame location is lower, and the conclusions depend on a simulation and thus are less direct than conclusions from nuclease digestion studies.

The simulation indicates that the preference for binding at each of the favored positions is about 5-fold higher than at other sites in the 208 bp unit (Figure 7a). There is no previous work with which this result can be directly compared. However, an earlier study using mononucleosomal templates suggested that nucleosome formation on the 208 bp 5S sequence is ∼1.6 kcal/mol more favorable than on random sequence DNA (*45*). Our simulation values would correspond to an ∼0.8 kcal/mol preference for any one of the three favored frames compared to nonfavored frames in the 5S unit. Although the two analyses involve somewhat different comparisons, the values are similar enough to suggest that our simulation-derived number may at least be in the correct range.

Nucleosome positioning in acetylated arrays was not analyzed in the earlier work. We find that acetylated nucleosomes also show preferential positioning within the 208 bp unit but some broadening of the site preferences. Thus, acetylation appears to have only a minor effect on positioning. In nuclease digestion studies, positioning in the 5S unit was reported to be unaffected by complete tail removal (*7*). With other positioning sequences, some loss in the efficiency but not in the location of positioning is observed when N-terminal histone tails are absent (*46*). All these results suggest that positioning is determined mainly by the globular portion of the nucleosome and that tails have at best only minor effects on positioning.

Second, nucleosomes apparently prefer to bind at DNA termini, by ∼10-fold, over binding at nontermini (Figure 7e,f). Acetylated or nonacetylated arrays show the tendency equally, suggesting that this preference also might not depend on the histone tails. That there is preferential binding to DNA termini in reconstituted chromatin has been known for some time (cf. *47*). Therefore, our AFM analysis independently detects another known feature of in vitro reconstituted chromatin, reinforcing the validity of the approach. Whether such end preferences have any physiological significance is not clear.

Third, in nonacetylated chromatin arrays, nucleosomes display a preference to locate close together on the DNA template. This cooperativity in template occupation is the most interesting and novel result from the AFM analysis. Scattered observations in the past have suggested cooperat-

ivity in nearest-neighbor nucleosome binding on DNA (cf. *45*, *48*), but the AFM results show the effect clearly. Because the effect is observed as an influence on the choices of DNA sites to which neighboring nucleosomes bind, we will refer to it as site−site cooperativity. Site−site cooperativity is absent when the N-terminal histone tails are acetylated. Therefore, these tails are required for the cooperativity, probably because they mediate the internucleosomal interactions that produce the cooperative effects. Since it is histone tail-mediated, this cooperativity is likely to be a general feature of chromatin and not restricted to this particular DNA template.

The tail-mediated interactions responsible for the cooperative effects probably include contacts between the tails and DNA, either linker or neighboring nucleosomal DNA, and histone−histone interactions (*40*, *41*, *49*), including tail−tail contacts. The occurrence of tail−tail interactions has been suggested from chromatin folding studies (reviewed in *49*). Nucleosome positioning in the 5S template is determined by the H3−H4 tetramer (*50*). These histones might also mediate the cooperativity. For example, in our hyperacetylated histones, acetylation resides almost entirely in the H3 and H4 tails (Yodh et al., unpublished results). Studies of histone partitioning during reconstitution suggest that the histone tails mediate an internucleosomal interaction worth ∼1 kcal/mol per nucleosome core (*51*). This value is virtually the same as the strongest cooperativity preference we observe (0−20 bp bin, Figure 7c). Both values are lower than the ∼2 kcal/mol per nucleosome estimated for the internucleosomal interaction by force studies of native chromatin fibers (*52*).

The N-terminal tails were not visualized in the nucleosome crystal structure (*40*), so their precise structural organization is unknown. If completely extended (random coil), the N-terminal portions of the histones that fall outside the globular core of the nucleosome would range in length from approximately 11 nm for H4 and H2B up to >14 nm for H3 (*41*, *44*, *49*). Subtracting 2 nm for the length of histone tail needed to traverse the DNA would leave ∼ 9 nm (H4/H2B) and ∼12 nm (H3) as the maximum possible extensions for tails from a single nucleosome. This corresponds to 21−24 nm between a neighboring pair of nucleosomes. The most distant cooperative effects that we observe involve nucleosomes that are separated by ∼40−60 bp (14−21 nm) on the DNA template (Figure 7c) and thus do fall within the possible contact range of these N-termini. However, it has been suggested that the H3 and H4 tails contain α-helical regions (*53*), which of course would shorten the projection length by an amount estimated to be ∼20% (*54*). On the other hand, bending of the linker DNA between nucleosome neighbors would shorten the distances that the tails must span in order to mediate internucleosomal contact. Thus, even the longest range cooperative effects that we observe are consistent with known properties of the histone tails. Another study that probably indicates the extension range of the histone tails observed that the core nucleosome can cause a major reduction in transcription factor DNA binding in regions 20 bp or more beyond the normally protected core nucleosomal domain (*55*). This corresponds to 40 bp or more between nucleosome neighbors, which is completely consistent with at least the medium-range (∼20−40 bp) cooperative effects that we observe (Figure 7c). The shortest range cooperative effects (0−7 nm, Figure 7c) probably include histone−histone contacts involving the shorter tails and/or tail−DNA (neighboring nucleosome) interactions, thus accounting for their enhanced strength.

Population analysis has demonstrated that nucleosome occupation of the 208-12 template is a multistate process and therefore not (highly) cooperative (*33*). There are at least two explanations to reconcile the apparent lack of cooperativity in a population analysis compared to the cooperative effects described in this locational analysis. First, the cooperative effects may simply be too small to produce detectable effects on a population distribution, which is likely to be dominated by the energetics of the basic histone−DNA interaction and therefore less sensitive to secondary effects such as cooperativity. In addition, if cooperativity were of the closed pair type, i.e., a pair of nucleosomes can form strong contacts with each other but only weak (or no) contacts with a third nucleosome, it would not propagate beyond individual pairs. For example, this trait is consistent with the lack of loading-level dependence observed in the location data (see above). The presence of such closed-pair interactions might be expected to appear in the population distribution as an absolute preference for occupation in even-numbered pairs, i.e., 2, 4, 6, 8, etc. No such absolute preference is observed (*61*). However, the locational analysis offers a possible explanation for this absence; the enhanced preference for nucleosomes to bind to DNA termini could enable enough binding of single nucleosomes at the ends to obscure the pair preference in population distributions. Further analyses to resolve these issues are underway. We note that both the 208-12 (*33*) and 172-12 (*61*) population distributions show a depletion in the frequency of molecules containing one nucleosome more or less than the major peak in the distribution, which leads to a weak *relative* pairwise preference. However, this feature is present whether the major peak is odd or even, and the behavior is actually enhanced in acetylated compared to nonacetylated chromatin arrays and thus is not likely to be due to internucleosomal interactions.

Cooperative effects should be important in the chromatin folding (compaction) process. Folding is usually considered to involve internucleosomal interactions between nucleosomes lying some distance apart on the DNA, with the intervening linker DNA and/or the higher order structure arranged in some fashion to allow the nucleosome−nucleosome contact. Our AFM results reflect a preference for nucleosome occupation of DNA sites that lie close together on the DNA template and do not reflect or include internucleosomal contact due to higher-order folding. Nor did we look for this type of contact because the potentially strong influence of surface forces in tapping-mode AFM may not allow such conformational features to be represented reliably. As is the case for site−site cooperativity, chromatin folding is mediated by the N-terminal histone tails and is inhibited by acetylation (*10*, *13*). Thus, site−site cooperativity and folding could involve the same intrinsic set of cooperative, tail-mediated internucleosomal interactions and thus reflect two aspects of the same basic effect. For example, sedimentation studies have identified a moderately folded higher-order conformation that requires only H3/H4 N-termini to form while the fully folded conformation requires the entire complement of tails (*15*, *49*). The partial set of tail-mediated

interactions that stabilize the moderately folded conformation may be the same ones responsible for the longer-range site−site cooperative effects we observe while the fully folded conformation and the close-range (0−7 nm) effects (Figure 7c) require the complete set of tail-mediated contacts. The occupational preference for two nucleosomes to lie close to one another, i.e., site−site cooperativity, should be able to nucleate a chromatin folding process better than separated nucleosomes. Thus, site−site cooperativity, particularly involving the longest range effects, might play an important role in initiating folding.

Nucleosome positioning and site−site cooperativity are two major features that determine internal nucleosome locations on the 208-12 template. These two influences may have a complex interplay. For example, site−site cooperativity between nucleosomes 0−20 bp apart on this template requires that at least one of the nucleosomes in the interacting pair lies outside a preferred binding position in the 208 bp unit. The relative magnitudes of the simulation values indicate that the cooperativity effects for such close contact are stronger than any positioning preference (Figure 7c versus 7a) and thus would be capable of overcoming the positioning preference for one of the nucleosomes in the interacting pair. On the other hand, for the longer-range (∼20−40, ∼40−60 bp) cooperative effects, the multiplicity of preferred positioning frames on the 5S template creates numerous ways that two nucleosomes can each lie in a preferred position within a 208 bp unit but still be close enough for these longer range interactions. For example, positioning of nucleosome *x* in frame 60−206 and nucleosome $x + 1$ in frame 20−166 would place this pair just over 20 bp apart, well within the range of cooperative effects (Figure 7c). In such a case, positioning preferences could facilitate cooperative interactions, by lowering the entropic barriers to bringing nucleosomes close enough for contact. On DNA that does not position nucleosomes, site−site cooperative effects involving very close-contacting nucleosomes would not ever have to compete, thermodynamically, with positioning preferences, as on the 208-12, but of course positioning preferences would also not be able to help facilitate the longer range cooperative effects. On nonpositioning DNA, it seems likely that the average internucleosomal length (repeat length) would play a major role in the overall extent of site−site cooperativity. Also, especially in longer repeat length chromatins, nucleosome sliding events could greatly alter the cooperativity in particular chromatin regions. Sequences that can position nucleosomes are thought to constitute a minor fraction within most genomes (*55*). However, locations where positioning sequences are repeated, such as in the case of certain DNA satellites, for example, could serve important roles as nucleation sites for large-scale folding in such genomes.

Salt gradient dialysis reconstitution is thought to produce nucleosomal distributions that reflect equilibrium conditions (*45*, *57*). Thus, cooperativity in nucleosome occupation should be an inherent thermodynamic property of chromatin and not an artifact of kinetic trapping processes. Cooperative effects could have important consequences for chromatin assembly associated with in vivo DNA replication. Newly synthesized histones are acetylated before being assembled into chromatin (cf. *3*, *36*, *58*, *59*). The absence of cooperativity in acetylated arrays would have the effect of keeping newly assembled nucleosomes independent and noninteracting in the early stages of chromosome assembly. The binding of regulatory proteins to their recognition sites and the resulting process of determination, i.e., establishing the patterns of gene regulation and chromatin structure in daughter genomes, might be easier to accomplish while individual nucleosomes behave independently, i.e., while they are acetylated, before the mature chromatin structure is in place. Among other things, the maturation process sets the final nucleosome repeat length. Remodeling factors that establish nucleosome spacing might also be able to function more efficiently on chromatin templates in which nucleosomes are independent (acetylated). Association of histone deacetylases with remodeling factors could thus create a complex that spaces nucleosomes appropriately and then "fixes" the mature repeat length, by deacetylating the chromatin template. At least one remodeling complex, NURD, is known to be associated with histone deacetylase activity (cf. *60*). After the newly assembled histones are deacetylated, cooperativity effects could contribute further to the maturation process by helping to nucleate the appropriate higher-order folded structures, dependent upon DNA positioning sequences, locations and levels of linker histones, local ionic environments, etc.

Cooperative effects should also have consequences for transcription. Such effects would help to keep nonacetylated arrays compacted but would not do so when nucleosomes are acetylated, thus loosening these arrays and allowing the nucleosomes to behave independently. Transcription-associated nucleosome remodeling, transcription factor binding, and RNA polymerase action would probably all be easier on noncooperative, acetylated nucleosome arrays. Sedimentation studies have demonstrated directly that acetylation induces array unfolding (*13*, *49*); acetylation (*34*−*39*) and array unfolding (*19*, *20*, *49*) are both associated with gene activation. The two major effects analyzed in this work, sequence-dependent positioning and cooperativity, are tendencies that contribute to determining the structure of nucleosomal arrays, the basic components of chromosomal organization. In cells, these features are combined with other features such as ionic milieu, linker histones, and nonhistone proteins to determine the overall chromosomal structure. It is this composite mix of features that makes chromatin such a complex entity, capable of a diversity of structural motifs and able to respond in various ways to a multitude of biological signals.

ACKNOWLEDGMENT

We thank Stuart Lindsay for helpful discussions.

REFERENCES

1. Lohr, D., Tatchell, K., and Van Holde, K. (1977) *Cell 12*, 829−836.
2. Martin, D., Todd, R., Lang, D., Pei, P., and Garrard, W. (1977) *J. Biol. Chem. 252*, 8269−8277.
3. van Holde (1989) *Chromatin*, Springer-Verlag, New York.
4. Bash, R., and Lohr, D. (2001) *Prog. Nucleic Acid Res. Mol. Biol. 65*, 197−259.
5. Simpson, R., Thoma, F., and Brubaker, J. (1985) *Cell 42*, 799−808.
6. Simpson, R., and Stafford, D. (1983) *Proc. Natl. Acad. Sci. U.S.A. 80*, 51−55.

7. Dong, F., Hansen, J., and van Holde, K. (1990) *Proc. Natl. Acad. Sci. U.S.A. 87*, 5724−5728.
8. Meerseman, G., Pennings, S., and Bradbury, E. (1991) *J. Mol. Biol. 220*, 89−100.
9. Hansen, J., van Holde, and Lohr, D. (1991) *J. Biol. Chem. 266*, 4276−4282.
10. Fletcher, T., and Hansen, J. (1996) *Crit. Rev. Eukaryotic Gene Expression 6*, 149−188.
11. Hansen, J., Ausio, J., Stanik, V., and van Holde, K. (1989) *Biochemistry 28*, 9129−9136.
12. Garcia-Ramirez, M., Dong, F., and Ausio, J. (1992) *J. Biol. Chem. 267*, 19587−19595.
13. Garcia-Ramirez, M., Rocchini, C., and Ausio, J. (1995) *J. Biol. Chem. 270*, 17923−17928.
14. Fletcher, T., and Hansen, J. (1995) *J. Biol. Chem. 270*, 25359−25362.
15. Tse, C., and Hansen, J. (1997) *Biochemistry 36*, 11381−11388.
16. Howe, L., Iskandar, M., and Ausio, J. (1998) *J. Biol. Chem. 273*, 11625−11629.
17. Carruthers, L., Bednar, J., Woodcock, C., and Hansen, J. (1998) *Biochemistry 37*, 14776−14787.
18. Carruthers, L., and Hansen, J. (2000) *J. Biol. Chem. 275*, 37285−37290.
19. Hansen, J., and Wolffe, A. (1992) *Biochemistry 31*, 7977−7988.
20. Hansen, J., and Wolffe, A. (1994) *Proc. Natl. Acad. Sci. U.S.A. 91*, 2339−2343.
21. Tse, C., Sera, T., Wolffe, A., and Hansen, J. (1998) *Mol. Cell. Biol. 18*, 4629−4638.
22. Sogo, J., Stahl, H., Koller, T., and Knippers, R. (1986) *J. Mol. Biol. 189*, 189−204.
23. Lohr, D., and Torchia, T. (1988) *Biochemistry 27*, 3961−3965.
24. Lohr, D. (1997) *J. Biol. Chem. 272*, 26795−26798.
25. Lyubchenko, Y., Jacobs, B., Lindsay, S., and Stasiak, A. (1995) *Scanning Microsc. 9*, 705−727.
26. Lyubchenko, Y., Gall, A., and Shlyakhtenko, L. (2001) *Methods Mol. Biol. 148*, 569−578.
27. Leuba, S., Yang, G., Robert, C., Samori, B., van Holde, K., Zlatanova, J., and Bustamante, C. (1994) *Proc. Natl. Acad. Sci. U.S.A. 91*, 11621−11625.
28. Martin, L., Vesenka, J., Henderson, E., and Dobbs, D. (1995) *Biochemistry 34*, 4610−4616.
29. Fritzsche, W., and Henderson, E. (1997) *Scanning 19*, 42−47.
30. Zlatanova, J., Leuba, S., and van Holde, K. (1998) *Biophys. J. 74*, 2554−2566.
31. Allen, M., Dong, X., O'Neill, T., Yau, P., Kowalczykowski, S., Gatewood, J., Balhorn, R., and Bradbury, E. (1993) *Biochemistry 32*, 8390−8396.
32. Sato, M., Ura, K., Hohmura, K., Tokumasu, F., Yoshimura, S., Hanaoka, F., and Takeyasu, K. (1999) *FEBS Lett. 452*, 267−271.
33. Yodh, J., Lyubchenko, Y., Shlyakhtenko, L., Woodbury, N., and Lohr, D. (1999) *Biochemistry 38*, 15756−15763.
34. Jeppesen, P., and Turner, B. M. (1993) *Cell 74*, 281−289.
35. Braunstein, M., Rose, A., Holmes, S., Allis, C., and Broach, J. (1993) *Genes Dev. 7*, 592−604.
36. Brownell, J., and Allis, C. (1996) *Curr. Opin. Genet. Dev. 6*, 176−184.
37. Roth, S., and Allis, C. (1996) *Cell 87*, 5−8.
38. Grunstein, M. (1997) *Nature 389*, 349−352.
39. Turner, B. (1991) *J. Cell Sci. 99*, 13−20.
40. Luger, K., Mäder, A., Richmond, R., Sargent, D., and Richmond, T. (1997) *Nature 389*, 251−260.
41. Luger, K., and Richmond, T. (1998) *Curr. Opin. Genet. Dev. 8*, 140−146.
42. Workman, J., and Kingston, R. (1998) *Annu. Rev. Biochem. 67*, 545−579.
43. Lyubchenko, Y., Shlyakhtenko, L., Harrington, R., Oden, P., and Lindsay, S. (1993) *Proc. Natl. Acad. Sci. U.S.A. 90*, 2137−2140.
44. Wolffe, A., and Hayes, J (1999) *Nucleic Acids Res. 27*, 711−720.
45. Shrader, T., and Crothers, D. (1999) *Proc. Natl. Acad. Sci. U.S.A. 86*, 7418−7422.
46. Polach, K., Lowary, P., and Widom, J. (2000) *J. Mol. Biol. 298*, 211−223.
47. Linxweiler, W., and Horz, W. (1984) *Nucleic Acids Res. 12*, 9395−9413.
48. Hansen, J., and Lohr, D. (1993) *J. Biol. Chem. 268*, 5840−5848.
49. Hansen, J., Tse, C., and Wolffe, A. (1998) *Biochemistry 37*, 17637−17641.
50. Dong, F., and van Holde, K (1991) *Proc. Natl. Acad. Sci. U.S.A. 88*, 10596−10600.
51. Widlund, H., Vitolo, H., Thiriet, C., and Hayes, J. (2000) *Biochemistry 39*, 3835−3841.
52. Cui, Y., and Bustamante, C. (2000) *Proc. Natl. Acad. Sci. U.S.A. 97*, 127−132.
53. Baneres, J., Martin, A., and Parello, J. (1997) *J. Mol. Biol. 273*, 503−508.
54. Wang, X., Moore, S., Laszckzak, M., and Ausio, J. (2000) *J. Biol. Chem. 275*, 35013−35020.
55. Thiriet, C., and Hayes, J. (1998) *J. Biol. Chem. 273*, 21352−21358.
56. Lowary, P., and Widom, J. (1997) *Proc. Natl. Acad. Sci. U.S.A. 94*, 1183−1188.
57. Lowary, P., and Widom, J. (1998) *J. Mol. Biol. 276*, 19−42.
58. Gruss, C., and Sogo, J. M. (1992) *Bioessays 14*, 1−8.
59. Annunziato, A. T., and Hansen, J. C. (2000) *Gene Expression 9*, 37−61.
60. Ng, H., and Bird, A. (2000) *Trends Biochem. Sci. 25*, 121−126.
61. Bash, R. C., Yodh, J., Lyubchenko, Y., Woodbury, N., and Lohr, D. (2001) *J. Biol. Chem. 276*, 48362−48370.

BI011612E